Multi-Sensor Characterization of the Boreal Forest: Initial Findings

Ernest Reith, Dar A. Roberts, and Dylan Prentiss
Department of Geography, University of California, Santa Barbara, CA 93106
ereith@aol.com

Abstract: Results are presented in an initial apriori knowledge approach toward using complementary multi-sensor multi-temporal imagery in characterizing vegetated landscapes over a site in the Boreal Ecosystem-Atmosphere Study (BOREAS). Airborne Visible/InfraRed Imaging Spectrometer (AVIRIS) and Airborne Synthetic Aperture Radar (AIRSAR) data were segmented using multiple endmember spectral mixture analysis and binary decision tree approaches. Individual date/sensor land cover maps had overall accuracies between 55.0% - 69.8%. The best eight land cover layers from all dates and sensors correctly characterized 79.3% of the cover types. An overlay approach was used to create a final land cover map. An overall accuracy of 71.3% was achieved in this multi-sensor approach, a 1.5% improvement over our most accurate single scene technique, but 8% less than the original input. Black spruce was evaluated to be particularly undermapped in the final map possibly because it was also contained within jack pine and muskeg land coverages.

Keywords: Multi-sensor, land cover, AIRSAR, AVIRIS, BOREAS.

Introduction

The northern boreal forest is important due to its sensitivity to changes in the physical climate system. Concern exists among some researchers that the boreal forest's current status as a carbon sink may be reversed due to changes in climate, vegetation succession patterns, fire frequency and the warming and drying of soils (Tans, et al., 1990). Timely and accurate land cover inventories are necessary for multi-scale modeling of climate change, carbon balance, energy flux, biodiversity, and wildfire. Promising results have been presented in the ability of various spectral imaging sensors and synthetic aperture radar (SAR) to produce land cover information over the boreal forest (Moghaddam and Saatchi, 1995; Ranson, et al., 1995, 1997; Hall, et al., 1997; Saatchi and Rignot, 1997).

Our premise is that we will achieve a higher overall accuracy in producing a land cover map using multiple sensor imagery over a season than from a single date, single sensor image. We present an non-automated, apriori knowledge approach based up data overlay to categorize a boreal forest site in Saskatchewan, Canada using multi-temporal, multi-sensor imagery. We attempt to characterize to a landscape level and compare it to a map produced by the Saskatchewan Environmental and Resource Management, Forest Branch – Inventory Unit (SERM-FBIU) using traditional photogrammetric methods. Airborne Synthetic Aperture Radar (AIRSAR) and Airborne Visible-InfraRed Imaging Spectrometer (AVIRIS) data were acquired over the BOReal Ecosystem-Atmosphere Study (BOREAS) Old Jack Pine (OJP) site in April, July, and September 1994. Land cover inputs for the overlay process were derived from AIRSAR-based binary decision trees (BDT) and AVIRIS-based multiple endmember spectral mixture analysis (MESMA) (Roberts, et al., 1998). The final land cover map was then evaluated against the SERM-FBIU data. A combination of a multi-sensor land cover map at 80% overall accuracy and a 10% improvement (80/10) from the best single source land cover map would be considered successful.

Study Area

The OJP site is located approximately 100 km northeast of Prince Albert, Saskatchewan. A 7 km x 5 km area containing the OJP site was selected within Nipawin Provincial Park, centered approximately at 521000mE, 5973000mN (North American Datum 1927, Universal Transverse Mercator Grid Zone 13). The topography of the site is flat with depressions occurring along drainage features.

A classification scheme was developed based on dominant landscape types in the existing SERM-FBIU validation data. The vegetative landscape is predominantly black spruce (*Picea mariana*) and jack pine (*Pinus banksiana*). Jack pine are common on well-drained, upland sandy brunisolic soils (Halliwell and Apps, 1997a). Stands of black and white spruce (*Picea glauca*) tend toward poorly drained sites. Deciduous trembling poplar or quaking aspen (*Populus tremuloides*) and tamarack (*Larix laricina*) are also found within the study area. Local grassy wetlands or fens are areas of inundation containing sedge vegetation (*Carex spp.*). Muskeg is a landscape marked by sparse stands of wet conifers such as jack pine and tamarack in areas of standing water.

Data Sources

The SAR data were collected by the JPL AIRSAR, a polarimetric, three-channel (C-, L-, and P-band) SAR operating onboard a reconfigured DC-8 aircraft. We evaluated data from three different dates over the 1994 growing season: leaf-off acquisition on April 28 (CM5575), maximum leaf-out scene on July

21 (CM5501), and pre-leaf drop data on September 20 (CM5381). All AIRSAR data acquisition were acquired while flying on a 341◈ heading (with respect to true north) at altitudes between 7473-7698 m above ground level (AGL). The area of interest was contained within incidence angles between approximately 25◈ in near range and less than 50◈ in far range in all cases. Cross track (range) and along track (azimuth) pixel resolutions were approximately 6.66 m and 9.26 m respectively.

The optical component of the study, AVIRIS, is a 224 channel, 10 nm spectral resolution imaging spectrometer flown in a NASA ER-2. A spatial resolution of approximately 20 m x 20 m is achieved when the platform is operating at 20 km altitude. The 1994 AVIRIS configuration acquired data over a spectral range between 373-2503 nm. AVIRIS data were collected on April 19 (940419, run 7, scene 4), July 21 (940721, run 7, scene 4), and September 16 (940916, run 8, scene 4). Data were acquired at local noon +/- one hour.

SAR Processing

The AIRSAR data were decompressed, retaining dB pixel attributes, and displayed in SAR slant range using ENVI 3.2 (ENVI, 1999). A 684 x 549 pixel sub set was selected to reduce storage requirements. Three polarizations (hh, vv, and hv) and total power (tp) were formed for each of the three channels. Four biomass-sensitive ratio images (c-hv/p-hv, c-hh/p-hh, l-hh/l-hv, p-hh/p-hv) were also produced to assist in differentiating between vegetated land cover types. Masks of land cover types are required to generate decision rules for the BDT. Each AIRSAR image was interpreted using traditional techniques of spatial relationships, texture, tone, pattern, and size keys and compared against its AVIRIS counterpart to determine candidate backscatter pixels for use in the BDT. Single, 2x2, and 3x3 pixel windows were collected and aggregated to create the necessary digital land cover masks. A minimum of 50 total pixels per land cover type per image were selected. Every attempt was made to co-locate training data across the three dates.

Water features and open/bare areas were identified by regions of low backscatter. The temporal nature of the data provided information regarding location of possible fens. Fens tended to be specular or very low backscattering characteristics in all wavelengths and polarizations prior to sedge growth in the April data. An indication of sedge growth was produced as shortwave, C-band backscatter increased in July and September. Jack pine stands required four separate training types based on different levels of volume scattering and open areas present. Low backscatter in very young jack pine stands reflected both the thin trunk and low foliage characteristics identified in those sites. Greater volume scattering was identified in regenerated, slightly older jack pine sites. Two types of mature jack pines were separated: thick and thin stands. Ample crowns produced greater volume scattering in both stand types. Thicker jack pine stands were distinguished from thin stands by a slight (~4 dB average between classes) increase in L-band Total Power (l-tp). Backscatter increased in areas of greater tree spacing due to bare surface-trunk double bounce mechanisms.

SAR speckle was reduced using a traditional 5x5 median filter on each of the three images prior to determining the BDT rules. Land cover masks were then run through a binary decision tree using S-PLUS against the filtered 16 bands of AIRSAR data (Chambers and Hastie, 1992). The decision tree output used a measure of heterogeneity termed deviance to calculate decision rules. The tree also identified influences that particular channels and polarizations had on specific land cover types (Safavian and Landgrebe, 1991). Each tree was evaluated to determine candidate branches for retention and removal. Branches with a small number of points, minimal increases in accuracy, or with redundant branches were pruned. A contingency matrix was produced to provide a relative indication of how well each training set compared to itself. Rules from each of the edited rule sets were placed into an Interactive Data Language (IDL) land cover categorization algorithm. The land cover maps were reduced (i.e. young jack pine, regenerated jack pine, thin jack pine, and thick jack pine = jack pine) to a categorization scheme similar to the SERM-FBIU evaluation data: aspen, black spruce, fen, jack pine, muskeg, open, tamarack, and water.

AVIRIS Processing

The AVIRIS data were transformed to apparent reflectance using a modified MODTRAN technique developed by Green et al. (1993). Radiance was inverted using water vapor look-up tables to upwelling measured radiance through non-linear least squares spectral fitting. Best-fit models were calculated for each individual pixel. Surface reflectance for each pixel was determined through an approach used by Roberts et al. (1997a). Adjustments to the modeled reflectance were made based on a ground calibration site in an AVIRIS frame near Prince Albert (940721 run 2, scene 2). The image cube was

reviewed for uncorrectable atmospheric scattering and absorption effects. Forty-five AVIRIS bands were removed from the original 224, leaving 179 to be used in the land cover mapping process.

Endmember spectra were collected directly from the AVIRIS image since no field-based spectra were collected at the OJP site. Temporally and near-temporally coincident large-scale color infrared airphotos and descriptions from a Natural Resources Canada-Canadian Forest Service (NRC-CFS) BOREAS document (Halliwell and Apps, 1997b) were used to locate cover types. Single and 2x2 pixel windows were used within ENVI to collect image spectra from the image cube. We attempted to acquire spectra from the same locations in each of the scenes.

Stands of aspen, tamarack, and fens were easily identified through time series analysis as they developed over the growing season. Seasonal leaf-off/leaf-on spectral signature provided adequate spatial reference for collecting aspen and tamarack spectra and backscatter. Leaf-on aspen in July had the highest reflectance values of the vegetation at the site, followed closely by sedge in the fen. Jack pine and black spruce spectra were difficult to separate. This might have been due to the fact that image endmembers reflected either a mixed stand or areas where spectral influences of the background diluted the purity of the pixel. High near infrared (NIR) reflectance in an apparently open field in the southern region provided additional evidence substantiating ancillary information that young jack pine had recently been planted. Muskeg was a difficult spectra to obtain because the amount and quality of resident stands differed spatially. White spruce is uncommon at the site and was difficult to collect a pure endmember.

One hundred and one image endmember spectra were collected according to the categorization scheme discussed above. These spectra were then visually compared to assess representative spectra for each scene's land cover types. Between 71 (940419) and 76 (940916) spectra were retained for use in our primary spectral mixture analysis procedure. Up to 40% of the endmembers were used to model jack pine.

Multiple endmember spectra were then compared to an AVIRIS scene using spectral mixture analysis 2-endmember methodology (Roberts, et al., 1997b). Mixing model criteria established root mean square (RMS) error and residual values exceeding 2.5% and 7 as non-candidate land cover estimates. The RMS output was then evaluated by determining the lowest RMS (if within other given constraints) and the optimal mixing model. An output image from the mixing model was then translated into a land cover map and reviewed against the SERM-FBIU data. Black spruce was undermapped due its spectral similarity to jack pine. The models were optimized using an approach described by Roberts et al., (1997b), designed to preferentially select specialist (models that are specific to a certain species) over generalists (models that do not discriminate well between species). In this case, black spruce was given a higher priority over the other image endmembers. White spruce could not be unmixed, probably due to poor spectra selection or a lack of pure stands. The optimized mixing model outputs were remapped to reflect the eight land cover types discussed above and coregistered with the AIRSAR land cover maps.

Multi-sensor Overlay Rules

The coregistered AIRSAR and AVIRIS maps were compared individually to the SERM-FBIU data (Figure 1) for content accuracy. We observed discrepancies between our results and the validation information reflecting minimum mapping unit issues and change over time. Areal photographs provided strong evidence of mixed stands and small pockets of other species within regions mapped as a single cover type. An unknown amount of generalization had taken place in the SERM-FBIU data compilation. In addition, several temporal land cover changes had occurred since the SERM-FBIU map had been compiled. Approximately 10% of the area previously mapped as open were interpreted from AVIRIS and airphotos to be in different stages of jack pine regrowth. In addition, logging had subsequently removed stands of jack pine and aspen in other locations transforming those areas into open. The SERM-FBIU validation data were updated to reflect large area land cover changes based on our interpretation of available air photos. Quantifying an overall accuracy for the individual outputs was made difficult by the dynamic nature of young jack pine spread and open space reduction to the south of the OJP site over the seasonal period of 1994.

Results

Overall accuracies for the six different date/sensor land cover maps ranged from 55.0% (940916 AVIRIS) to 69.8% (940721 AVIRIS). Individual producer's accuracy was used to indicate what season/sensor combinations best identified the landscape at OJP (Table 1). No individual sensor or season played a significant role in providing a high accuracy land cover type to the decision rule. AIRSAR and AVIRIS imagery contributed four land cover types apiece. The 940419 AVIRIS data were the only

component of the time series imagery that did not produce a layer land cover to the multi-sensor data set. The 940721 AVIRIS scene contributed two classes (fen and jack pine) or a total of 204,697 pixels (54.4% of the site). Four land cover types (aspen, muskeg, open, and tamarack) were best identified using September data (940916 AVIRIS and 940920 AIRSAR). The best eight land cover layers from all dates and sensors correctly characterized 79.3% of the cover types when combined.

Table 1. Individual land cover type producer's accuracies

Land cover	Accuracy	Date	Sensor
Aspen	65.1%	940916	AVIRIS
Black Spruce	73.2%	940428	AIRSAR
Fen	70.8%	940721	AVIRIS
Jack Pine	81.1%	940721	AVIRIS
Muskeg	73.2%	940920	AIRSAR
Open	80.1%	940916	AVIRIS
Tamarack	33.5%	940920	AIRSAR
Water	77.5%	940721	AIRSAR

High NIR reflectance present in the 940721 and 940916 AVIRIS scenes was used to identify grassy fens and aspen stands. Evidence of aspen modeling healthy fens and tamarack stands occurred. 940721 AVIRIS was also used to detect fresh summer growth in jack pine. AIRSAR L- and P-bands were sensitive to the wet surfaces common to black spruce stands. In general, black spruce was undermapped and appeared to be confused with both jack pine stands and muskeg. It is possible that black spruce was contained within both of the cover types, but not as the dominant cover type. Double-bounce backscatter was critical in identifying muskeg located in the site. Water bodies and open areas were best modeled by spectra in the 940721 and 940916 AVIRIS data respectively. We would have expected AIRSAR to be sensitive to the specular surface component of both classes. Tamarack was not well modeled by either sensor or overmapped by SERM-FBIU. The double bounce mechanism in the wetlands was used to identify tamarack. Each cover type, excluding tamarack, is representative of accuracies achieved in other BOREAS imaging spectrometer research (Zarco-Tejada and Miller, 1999; Sandmeir and Deering, 1999).

A series of overlay procedures used the most accurate data layers from the time series imagery to produce a multi-sensor land cover map through a series of overlay processes (Figure 2). Commission error was used to determine overlay order. High commission error was given lowest priority and was the first layer. A second layer of open and tamarack from 940721 AVIRIS was included due to similar high accuracies.

An overall accuracy of 71.3% was achieved, only a 1.5% increase over the best single scene - 940721 AVIRIS. Most of the individual cover type producer's accuracies were reduced after being transformed by the decision rule (Table 2). Black spruce accuracy was reduced by 37.6%. Black spruce was the first coverage placed by the process we followed, leaving competing coverages such as muskeg and jack pine to overlay black spruce. The initial accuracy of black spruce and muskeg was reduced when overlaid by overmapped pixels of jack pine. Aspen, open, tamarack, and water were placed toward the end of the decision rule process and were not subjected to being superceded. Most of the 14,780 unmodeled pixels (4% of the image) were open areas.

Table 2. Multi-sensor cover type producer's accuracies per land cover type

Land cover	Accuracy
Aspen	65.0%
Black Spruce	35.6%
Fen	64.6%
Jack Pine	79.7%
Muskeg	53.9%
Open	81.2%
Tamarack	33.0%
Water	77.5%

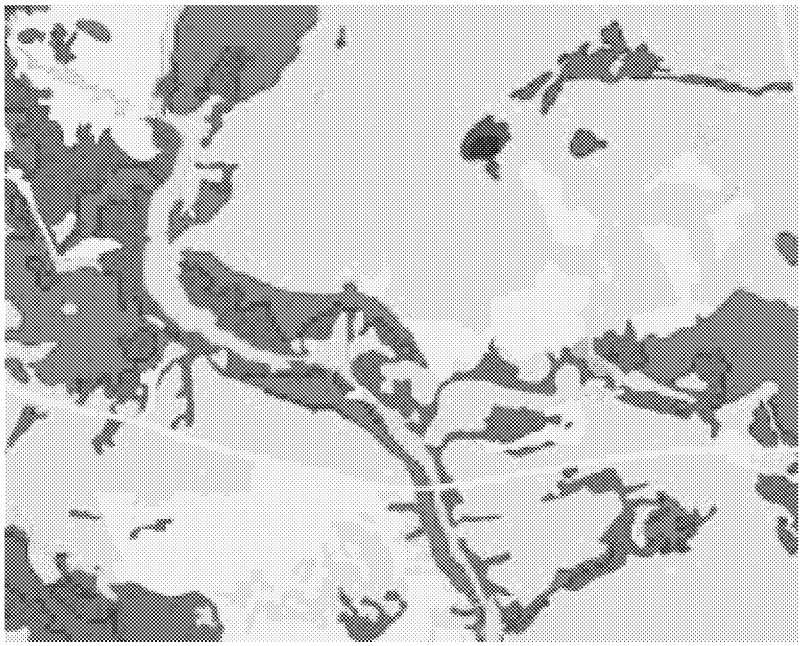

Aspen Black Spruce Fen Jack Pine Muskeg Open Tamarack Water Unmodeled

Figure 1. *SERM-FBIU OJP land cover map (without updated information).*

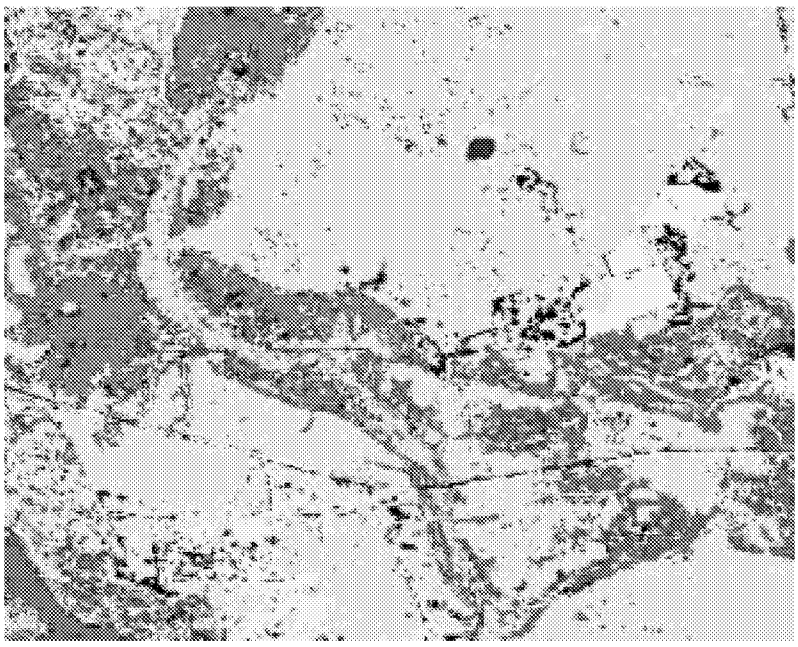

Aspen Black Spruce Fen Jack Pine Muskeg Open Tamarack Water Unmodeled

Figure 2. OJP multi-sensor land cover map (April-September 1994).

Conclusions and Recommendations

On a cover-by-cover basis, our initial assumptions of sensor sensitivity to a particular land cover types typically held. The three wet conifer dominate landscapes - black spruce, muskeg, and tamarack – exhibited high double-bounce-induced backscatter than the surrounding low growing fens and dry subsurface jack pine. The deciduous aspen and tamarack seasonal phenological patterns were evident in AVIRIS spectra. Fen was best identified using AIRSAR to distinguish the pre-growing season specular characteristic and then AVIRIS for the spectral component as vegetation developed. Water was separated due to its specular AIRSAR signature and was often confirmed by its lack of NIR spectral response. We would have expected AIRSAR to contribute more information regarding open areas than we actually derived from the AVIRIS spectra.

Neither the overall nor the improved accuracy approached our goal of 80/10. This result is due to an ill-constructed overlay where pixels representing errors of commission decreased the overall accuracy of the land cover map. The overall accuracy of the individually derived multi-sensor derived land cover data in Table 1 accurately represented 79.2% of the OJP site. The overlay procedure, as applied in this research, only provided a slight increase of 1.5% in overall accuracy over the best single sensor scene, while reducing the accuracy of the combined input data by 7%.

An 80/10 increase over the best single source map could be achieved if correctly evaluated pixels were masked out prior to a decision rule being constructed. The amount of unmodeled open pixels could be reduced with supplementary spectra being collected in brighter soil areas. In addition, incorrectly categorized pixels would then be evaluated using an enhanced decision rule approach evaluating ancillary images of non-photosynthetic vegetation (npv), green vegetation, or liquid water estimates derived from AVIRIS. These rules would possibly better segment the remaining incorrectly categorized pixels, while retaining already correctly identified data. Additional investigations will be made into combining AIRSAR and AVIRIS image sets into hyper-cubes for subsequent n-dimensional data visualization endmember collection procedures.

Acknowledgments

Much of the research was funded by the NASA-BOREAS grant NAG5-7248. The authors wish to thank the following data and software providers: BOREAS team; SERM-FBIU; NRC-CFS; Oak Ridge National Laboratory Distributed Active Archive Center; AIRSAR and AVIRIS teams; and Research Systems, Incorporated.

References

Chambers, J.M. and Hastie, T.J. (eds.) (1992), Statistical Models in S, Waldsworth and Brooks/Cole Advanced Books and Software, Pacific Grove, California, pp. 377-419.

ENVI 3.2 (1999), Better Solutions Consulting Limited Liability Company, Lafayette, Colorado, 864 p.

Green, R.O., Conel, J.E., and Roberts, D.A. (1993), Estimation of aerosol optical depth and additional atmospheric parameters for the calculation of apparent reflectance from radiance measured by the Airborne Visible/Infrared Imaging Spectrometer, in Green, R.O. (ed.) Summaries of the Fourth Annual JPL Airborne Geoscience Workshop, JPL Publication 93-26, Vol. 1, pp. 73-76, Washington, D.C., October 25-29, 1993.

Hall, F.G., Knapp, D.E., and Huemmrich, K.F. (1997), Physically based classification and satellite mapping of biophysical characteristics in the southern boreal forest, *Journal of Geophysical Research*, Vol. 102, No. D24, pp. 29,567-29,580.

Halliwell, D.H. and Apps, M.J. (1997a), BOReal Ecosystem-Atmosphere Study (BOREAS) biometry and auxiliary sites: soils and detritus data, Natural Resources Canada, Canadian Forest Service, Northern Forest Centre, Edmonton, Alberta, 235 p.

Halliwell, D.H. and Apps, M.J. (1997b), BOReal Ecosystem-Atmosphere Study (BOREAS) biometry and auxiliary sites: locations and descriptions, Natural Resources Canada, Canadian Forest Service, Northern Forest Centre, Edmonton, Alberta, 120 p.

Moghaddam, M. and Saatchi, S. (1995), Analysis of scattering mechanisms in SAR imagery over boreal forest: results from BOREAS '93, *IEEE Transactions on Geoscience and Remote Sensing*, Vol. 33, No. 5, pp. 1290-1296.

Ranson, K.J, Saatchi, S., and Sun, G. (1995), Boreal forest ecosystem characterization with SIR-C/XSAR, *IEEE Transactions on Geoscience and Remote Sensing*, Vol. 33, No. 4, pp. 867-876.

Ranson, K.J., Sun, G., Lang, R.H., Chauhan, N.S., Cacciola, R.J., and Kilic, O. (1997), Mapping of boreal forest biomass from spaceborne synthetic aperture radar, *Journal of Geophysical Research*, Vol. 102, No. D24, pp. 29,599-29,610.

Roberts, D.A., Green, R.O., and Adams, J.B. (1997a), Temporal and spatial patterns in vegetation and atmospheric properties from AVIRIS, *Remote Sensing of Environment*, Vol. 62, pp. 223-240.

Roberts, D.A., Gardner, M.E., Church R., Ustin, S.L., and Green, R.O. (1997b), Optimum strategies for mapping vegetation using multiple endmember spectral mixture models, Proceedings of SPIE, Vol. 3118, Imaging Spectrometry III, pp. 108-119, San Diego, California, July 27 – 1 Aug, 1997.

Roberts, D.A., Gardner, M., Church, R., Ustin, S., Scheer, G., and Green, R.O. (1998), Mapping chaparral in the Santa Monica Mountains using multiple endmember spectral mixture models, *Remote Sensing of Environment*, Vol. 65, pp. 267-279.

Saatchi, S.S. and Rignot, E. (1997), Classification of boreal forest cover types using SAR images, *Remote Sensing of Environment*, Vol. 60, pp. 270-281.

Safavian, S.R. and Landgrebe, D. (1991), A survey of decision tree classifier methodology, *IEEE Transactions on Systems, Man, and Cybernetics*, Vol. 21, No. 3, pp. 660-674.

Sandmeier, S. and Deering, D.W. (1999), Structure analysis and classification of boreal forest using airborne hyperspectral BRDF data from ASAS, *Remote Sensing of Environment*, Vol. 69, pp. 281-295.

Tans, P.P., Fung, I.Y., and Takahashi, T. (1990), Observational constraints on the global atmospheric CO_2 budget, *Science*, Vol. 247, pp. 1431-1438.

Zarco-Tejada, P.J. and Miller, J.R. (1999), Land cover mapping at BOREAS using red edge spectral parameters from casi imagery, in press.